DYNAMICAL MODELING AND SIMULATION OF THE FOUR-WHEEL MICRO ROVER IN SANDY TERRAIN

Takuto Oikawa [a], Nicolò Carletti [b], and Kazuya Yoshida[c]

[a] *Tohoku University, 6-6-01, Aramaki Aoba, Sendai, 980-8570, Japan, oikawa@astro.mech.tohoku.ac.jp*
[b] *Dipartimento di Scienze e Tecnologie Aerospaziali, Politecnico di Milano, Via La Masa, 34, Milan, 20156, Italy, nicolo.carletti@mail.polimi.it*
[c] *Tohoku University, 6-6-01, Aramaki Aoba, Sendai, 980-8570, Japan, yoshida@astro.mech.tohoku.ac.jp*

Abstract

With the arrival of low cost launch options, space exploration has become accessible and affordable, attracting many researchers and start-ups. This has led to more difficult mission opportunities, becoming possible for research organizations such as the development of resource prospecting rovers for environments such as the lunar surface. With this in mind, Tohoku University's "Space Robotics Laboratory", in collaboration with ispace, is currently developing a lunar rover for the Google Lunar XPRIZE competition, which aims to be used for resource prospecting in future mission. Uncertainties are inherent in space development as single point failures can hinder the rover's mobility performance in a space environment and lead to mission failure. One of the most important locomotive factors is the wheel-soil interaction under rough terrain with loose soil, where wheel slippage has been a recurring issue. Our objective is to enable straight traversal under sloped terrain. Given that drift is inevitable, a new locomotive method is proposed. This is essential for rover teleoperation to reach the destination as quickly and safely as possible.

In this paper, a simulator for dynamics of a four-wheeled vehicle is developed. The dynamics of the wheel are formulated based on well-known terramechanics theories. To match the model with the experimental data from the single wheel testing, we have tuned the parameters that are dominant elements in the equation, which is the shear deformation modulus. Once the wheel-soil characteristics are determined, the dynamic model is translated into the four-wheel rover case. We have performed several traversal runs on different inclined testbeds under controlled conditions to validate the simulator's accuracy. Furthermore, we have determined the straight horizontal traversal motion by orienting the rover's attitude for specific slopes, and we have evaluated its consistency with the experimental data.

Keywords: Dynamic modeling, Terramechanics, Lunar exploration, Four-wheel rover

1. Introduction

With the recent increase in the number of start-ups in the space industry, space has become accessible with opportunities for businesses and research. One new opportunity for private organizations is the Google Lunar XPRIZE (GLXP) challenge, where teams globally are competing for the title of first privately built space system to land and travel on the lunar surface. As the sole team from Japan, HAKUTO is designing a four-wheel vehicle (Fig. 1) that can survive the harsh lunar condition, and that has a mass of approximately 4.5 kg, which is a very light-weight vehicle for such a mission. Even with a low mass budget, this rover has proved capable on Earth of traversing long terrain and sending high definition images back from previous field test results. However, Bekker (1969) pointed out that the current established theories do not accurately predict the terrain performance of a low weight vehicle in a loose soil

condition. In fact, Kerr (2009) reported that the previous Mars rover's wheels buried itself into loose Martian soil and permanently became immobile. With the lunar regolith's interaction on the wheels at low mass load not being well-known, the rover could potentially threat similar issues as the Mars rover. Therefore, the rover's mobility performance needs to be examined carefully to assess its locomotive characteristics under sandy terrain.

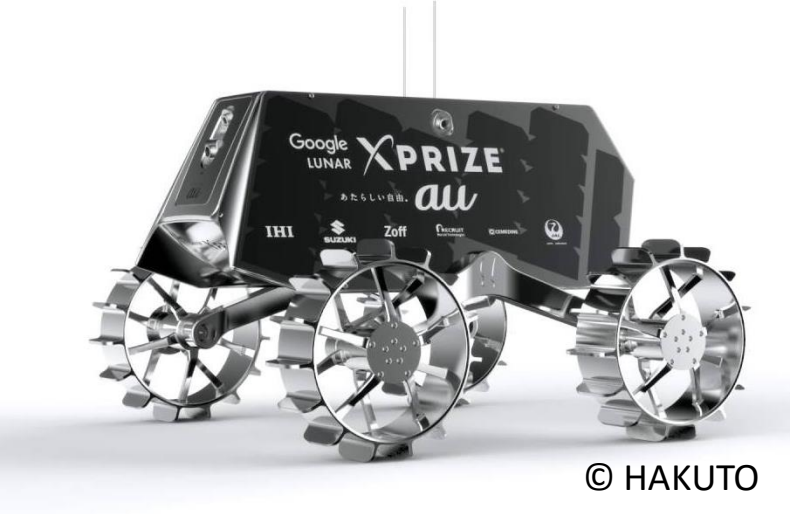

Fig. 1. *HAKUTO Flight Model Rover*

In the past research, dynamics simulations based on terramechanics studies are conducted both in single wheel testing (Irani et al, 2011) and rover platform (Li et al, 2013; Merion-Griffith and Spenko, 2014) to predict the mobility characteristics in sandy terrain. While the fore mentioned investigations focus on the dynamics, Nagaoka et al (2016) developed two different control techniques to compensate rover's traversal motion and demonstrated that the skid-steering method is more energy efficient for the rover when compared to a continuous circular maneuver to the same target destination. Whereas, Inotsume et al (2016) proposed an effective path route to ascend in a loose sloped soil.

In the actual mission, we plan to adopt a simple motion control such as forward and backward locomotion and spot turn just like Nagaoka et al's method (2016) for the most energy efficient strategy. The low-level complexity keeps the system robust, while reducing the amount of potential failure nodes from a software aspect. On the other hand, the passive locomotive control does not account for every possible mobile difficulty such as the horizontal traversal in a sloped terrain. In this paper, we simulate the mobility performance of the skid-steering type rover's dynamics and study passive attitude compensation for straight traversal run.

2. Dynamics Modeling and Equation of Motion

This section highlights the dynamics modeling formulation of the 4-wheel rover.

2.1 Reference Frame

To study the dynamics in the general case (when the rover is in a traversal run), we have defined three coordinate reference frames (Fig**.** 2), which are:

- Inertial reference frame (x_i, y_i, z_i): This is the fixed reference frame at origin. The x axis is aligned with the transversal direction of the slope, the y axis is in the longitudinal direction of the ground plane, and the z axis is in the absolute vertical direction.
- Horizon reference frame (x_h, y_h, z_h): This reference frame is obtained by rotating the x inertial axis at an specific inclination angle (α). This rotation aligns the y and z axis to the longitudinal direction and the normal of the inclined surface respectively.

- Body reference frame (x_h, y_h, z_h): This reference frame is fixed to the principal axis of inertia of the rover, where the x axis is in the locomotive direction.

For the computation related to the rover's dynamics and the wheel-soil interaction, the body reference frame is used.

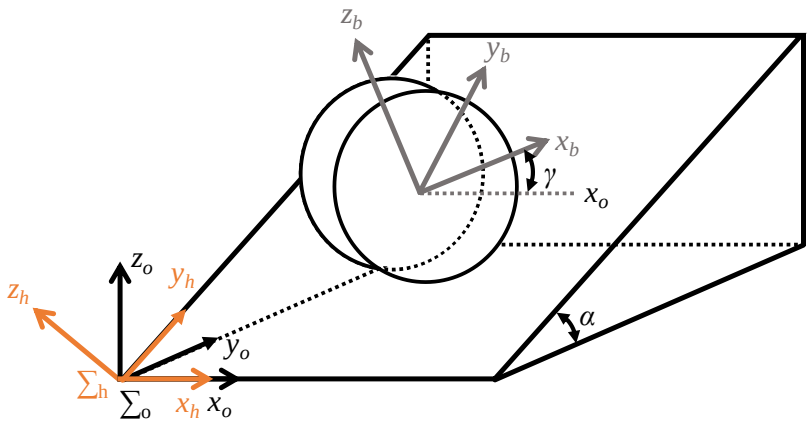

Fig. 2. *Global coordinate reference frame of the rover.*

2.2 Rover Dynamic Model

According to the structure and the mobility studied in this work, a set of premises are introduced to simplify the dynamic equations. The structure is considered rigid and any aerodynamic effect is neglected due to the vacuumed condition in an actual lunar mission. We assume that the rover has no damping mechanism. The rover has four integral motors, where each of them actuates the wheel independently. This enables spot turn maneuver by using skid steering. The only moving part in the rover is the joint in which the wheel arm are attached. This degree of freedom can be neglected for the model. Being that its purpose is to compensate rough terrain, this study encapsulates the dynamics only for flat terrain with certain inclination angle.

From these assumptions, five rigidly connected masses are developed: the main body (index 0) and the four wheels (index 1-4). Figure 3 illustrates the rover dynamic of five different components, where the system has 16 moving elements: longitudinal, lateral motion, and yaw (γ, shown in Fig. 2) motion for the bodies the wheels and the four wheels rotation (θ_i). Since the wheels only have one degree of freedom along the y-axis with no steering mechanism, we can treat all rotations along the z-axis as equal. To simplify the dynamics, the state vector ($\bar{x}$) incorporates only three states, the translation and rotation movement of the rovers, which is shown in Eq. 1.

$$\bar{x}_i = \begin{bmatrix} x_i & y_i & \gamma \end{bmatrix}^T \tag{1}$$

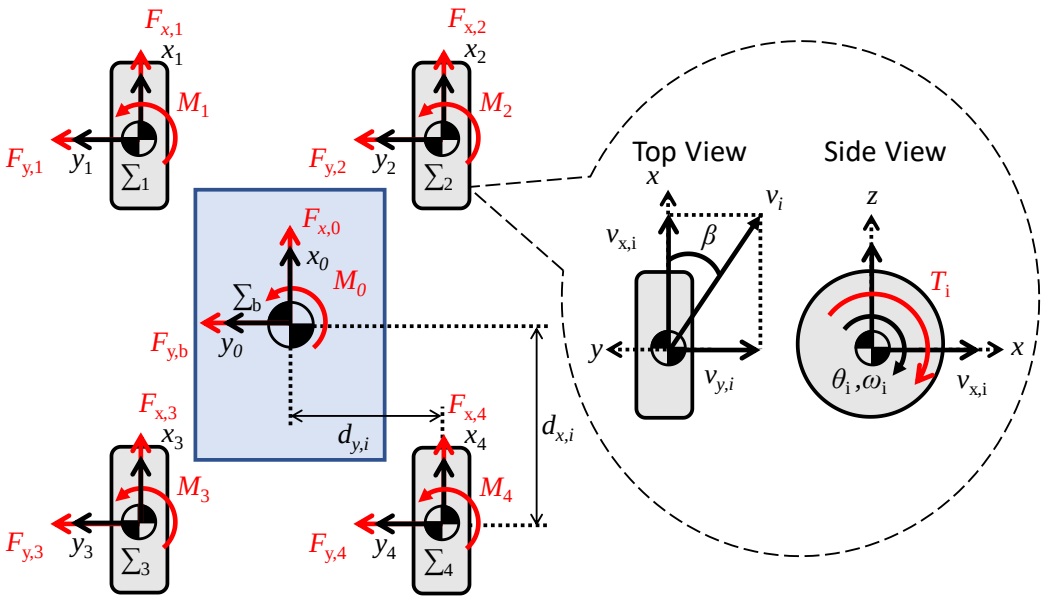

Fig. 3. *Simplified rover's structure and dynamics of equation of motion.*

Index i represents the translational degrees of freedom for each rover's components. Using Newtonian mechanics, the rover kinematics are derived,

$$\bar{x}_i = \bar{x}_{0,i} + \bar{A}\tilde{d}_i \tag{2}$$

$$\dot{\bar{x}}_i = \dot{\bar{x}}_{0,i} + \bar{A}\left(\bar{\Omega} \times \tilde{d}_i\right) \tag{3}$$

$$\ddot{\bar{x}}_i = \ddot{\bar{x}}_{0,i} + \bar{A}\left(\dot{\bar{\Omega}} \times \tilde{d}_i\right) + \bar{A}\left(\bar{\Omega} \times \left(\bar{\Omega} \times \tilde{d}_i\right)\right) \tag{4}$$

where $\bar{x}_{0,i}$ is the initial condition vector, $\bar{A}$ is the rotation matrix described by the angle γ, $\bar{\Omega}$ is the angular rotation vector ($[0\ 0\ \dot{\gamma}]^T$), $\tilde{d}_i$ is the constant distance vector from the center of mass to the corresponding elements. The forces (F_i) and moments (M_i) applied to each wheel pertain to the reactions from the soil-wheel interaction, which are then directly translated to the rover's overall motion. Furthermore, torques (T_i) are also applied to the wheels from the motor and the soil-wheel contact resistance moment. These external forces and moments are summed as resulting reactions to the body:

$$\begin{cases} F_{x,0} = \sum_{i=1}^{4} F_{x,i} + m_w \dot{\gamma}^2 \sum_{i=1}^{4} \left(d_{x,i} \times \cos\gamma + d_{y,i} \times \sin\gamma\right) \\ F_{y,0} = \sum_{i=1}^{4} F_{y,i} + m_w \dot{\gamma}^2 \sum_{i=1}^{4} \left(d_{x,i} \times \sin\gamma + d_{y,i} \times \cos\gamma\right) \\ M_0 = \sum_{i=1}^{4} \left(M_i + d_{x,i} \times F_{y,i} + d_{y,i} \times F_{x,i}\right) \end{cases} \tag{5}$$

where m_w is the mass of the wheel. With the rover being symmetrical along the x-axis, the equations of motions are set up using the principle of virtual work:

$$\bar{M}\ddot{\bar{x}}_i = \bar{F} \tag{6}$$

$$\overline{M} = \begin{bmatrix} m_{tot} & 0 & I_{xz} \\ 0 & m_{tot} & I_{yz} \\ I_{xz} & I_{yz} & I_{zz} \end{bmatrix} \tag{7}$$

$$I_{xz} = m_w \sum_{i=1}^{4} \left(d_{y,i} \times \cos\gamma + d_{x,i} \times \sin\gamma \right) \tag{8}$$

$$I_{yz} = m_w \sum_{i=1}^{4} \left(d_{x,i} \times \sin\gamma + d_{y,i} \times \cos\gamma \right) \tag{9}$$

$$I_{zz} = I_{b,zz} + 4I_{w,zz} + m_w \sum_{i=1}^{4} \left(d_{x,i}^2 + d_{y,i}^2 \right) \tag{10}$$

$$\overline{F} = \begin{bmatrix} F_{x,i} \\ F_{x,i} \\ M_i \end{bmatrix} \tag{11}$$

where $\overline{M}$ is the mass matrix of the rover (m_{tot} is the total mass of the rover and I is the moment of inertias) and $\overline{F}$ is the force/moment matrix of the rover. The masses, the moments of inertia of each component, and their corresponding position from the center of mass are obtained through a CAD model, shown in Table 1 and
Table 2.

Table 1. Rover's mechanical properties.

	m [kg]	I_{xx} [kgm^2]	I_{yy} [kgm^2]	I_{zz} [kgm^2]
Main Body	5.24	0.138	0.142	0.230
Wheel	0.422	0.00100	0.00154	0.00100

Table 2. Rover's center of mass position.

	x [m]	y [m]	z [m]
Main Body	0	0	0
Wheel 1	0.19	0.24	- 0.06
Wheel 2	- 0.17	0.24	- 0.06
Wheel 3	- 0.17	- 0.24	- 0.06
Wheel 4	0.19	- 0.24	- 0.06

2.3 Wheel Model for Sloped Terrain

In the case of a terrain with a certain inclination angle (α), a small adjustment is required to account for the gravitational pull on the longitudinal direction of the sloped surface. The transformation on the normal load (W) using trigonometric function is applied:

$$F_{x,slope} = W \sin\alpha \sin\gamma \tag{12}$$

$$F_{y,slope} = W \sin\alpha \cos\gamma \tag{13}$$

$$F_{z,slope} = W \cos\alpha \tag{14}$$

2.4 Slip Ratio

Owing to the condition under loose soil, a wheel moving on a sandy terrain has a certain amount of skid. Two parameters, the slip ratio (s) and the slip angle (β) are used as dynamic inputs for this study. The slip ratio is a relation between the wheel's radius (r), rotation velocity (ω), and the velocity of the ground (v_x). It is modeled as in Eq. 15.

$$s = \begin{cases} \dfrac{r\omega_i - v_x}{rw} & if\,|r\omega_i| > |v_x| \\ \dfrac{r\omega_i - v_x}{v_x} & if\,|r\omega_i| < |v_x| \end{cases} \tag{15}$$

If the grousers are considered and their number is high enough, another approach can be used. Considering that h_g is the height of the grousers, slip ratio defined by the previous equation is modified to the following:

$$s = \begin{cases} 1 - \dfrac{v_x}{(r+h_g)\omega_i} & if\,|(r+h_g)\omega_i| > |v_x| \\ \dfrac{(r+h_g)\omega_i}{v_x} - 1 & if\,|(r+h_g)\omega_i| < |v_x| \end{cases} \tag{16}$$

The lateral component of the slipping phenomenon is determined with the β, that is defined as the angle formed by the lateral component of the traveling velocity (v_y) and the longitudinal one (v_x):

$$\beta = \tan^{-1}\left(\frac{v_y}{v_x}\right) \tag{17}$$

3. Numerical Simulation Approach

Based on the formulated dynamics, a numerical simulation is performed to compute the rover's motion in sandy terrain. This simulator is developed from the need to characterize actual mobility performance in lunar surface condition, which is a challenge to replicate in a terrestrial environment. To justify the feasibility of the simulator, the dynamical response is compared with on-ground test results using known soil properties.

Among different control choices to regulate the rover's velocity, we have implemented speed control technique, imposing specific wheel velocity in a simple algorithm. To fit the numerical simulation at a target velocity (v_{des}), we introduce a reference slip ratio (s_{ref}) along with the slip ratio, wheel's radius, and the yaw heading to determine the new wheel rotation speed (Eqn. 18). Based on prior experimental work (Ishigami et.al., 2008) and other works on ground vehicle research (Fujii and Fujimoto, 2007), the s_{ref} is chosen at 0.2.

$$\omega_i = \frac{v_{des}}{(1-(s_{ref}-s))(r+h_g)\cos\gamma} \tag{18}$$

Figure 4 illustrates the control diagram of the rover model. At the initial input, the user chooses the desired states (target velocity and attitude) at which the rover is planned in motion. The state information is loaded into the slip controller to compute the instantaneous wheel rotation speed, defined by Eqn. 16. This value is then translated into the wheel-soil model to calculate the corresponding forces and torques applied to the wheels, followed by the dynamics model defined in previous section. The whole process is iterated until the rover reaches to the desired velocity. The wheel-soil interaction model is based on the established terramechanics theory derived by previous researchers (Bekker, 1960, 1969; Janosi and Hanamoto, 1961; Wong and Reece, 1967; Wong, 2008) and the proposed model to predict lateral forces (Ishigami et al 2007, 2009) and the grouser effect (Sutoh, 2013 and Sutoh et al, 2013) for sandy terrain.

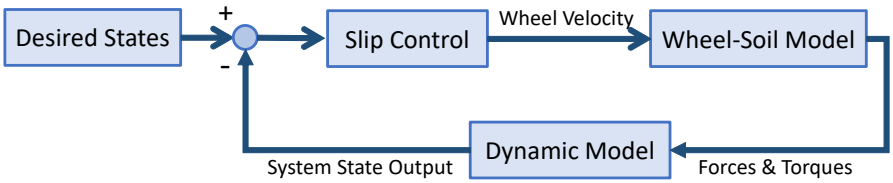

Fig. 4. *Speed control block diagram.*

Figure 5 shows the simulation flowchart of the four-wheel rover dynamics. There are two sets of determined constants to initialize the simulation. The first one is the geometric properties of the rover system, and the second is formed by the parameters to describe the ground conditions. For this study, the Toyoura sand is used, which properties are shown in Table 3.

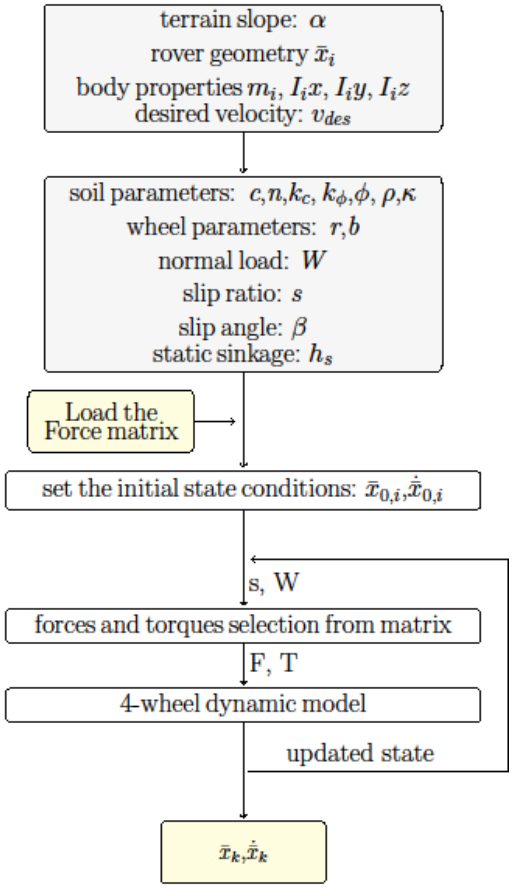

Fig. 5. *Numerical simulation flowchart.*

Table 3. Soil parameter.[a]

Parameter	Symbol	Value
Cohesion stress	c	0.0 kPa
Friction angle	ϕ	38.0°
Soil destructive angle	X_c	26.0°
Cohesive modulus	k'_c	0.0
Frictional modulus	k'_ϕ	1203.54
Longitudinal shear deformation modulus	K_x	0.036+0.043×β
Lateral shear deformation modulus	K_y	0.013+0.020×β
Sinkage exponent	n	1.703
Maximum stress angle modulus	a_0	0.40
Maximum stress angle modulus	a_1	0.15
Soil density	ρ	1490.0 kg/m^3

[a] Soil parameters are obtained from Ishigami (2009)

4. Single Wheel Test

4.1 Testbed Setup

To determine the validity of the model, we measured the forces applied on the wheel using the sandbox shown in Fig. 6. The equipment has two force torque (F/T) sensors, two encoders to measure the wheel's traveled distance and sinkage, and counter weight to simulate the actual weight applied on single wheel, which is about 20N of vertical force. With frictional effect along the linear guide rail and encoder's pull to the testing apparatus not being miniscule, we counterbalanced the effective drawbar pull of the wheel by varying pulley weights on both sides of the testbed. This effectively measures the forces applied onto the wheel with different slip conditions.

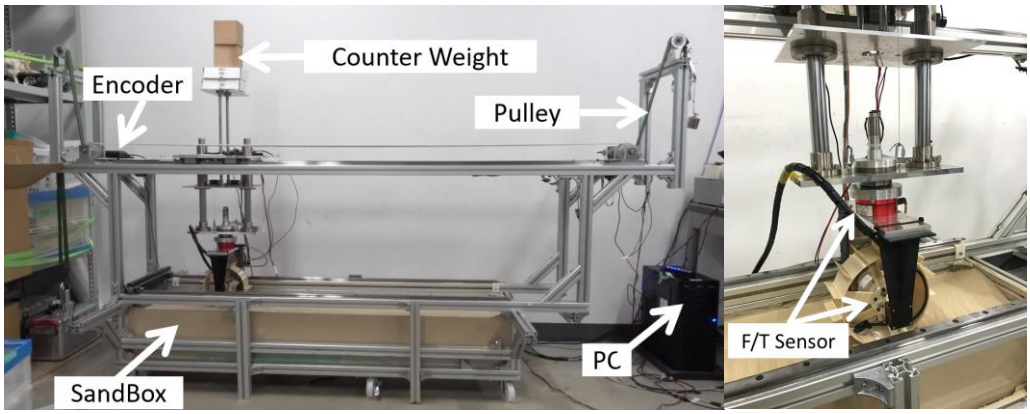

Fig. 6. *Single wheel testbed setup and apparatus.*

4.2 Test Results

Figure 7 shows the experimental result of both F_x and F_y with slip ratios from varying drawbar pull conditions. The wheel is tested at $\beta = 0°$, simulating straight run along the sandy surface. Based on the test, the overall graph tendency for both the model and experiment matches closely for F_y as no side slip is applied for the test. For the F_x, the model still overestimates the forces at high slip ratio condition using the Ishigami's parameter. This requires a slight tuning in the model, and we have chosen to modify the longitudinal shear deformation modulus from Janosi and Hanamoto's equation to 0.3 at y-intercept. Although this tuning does not match exactly with initial slip ratio forces, we have minimized the disparity between the model and the experimental result when compared to previous model.

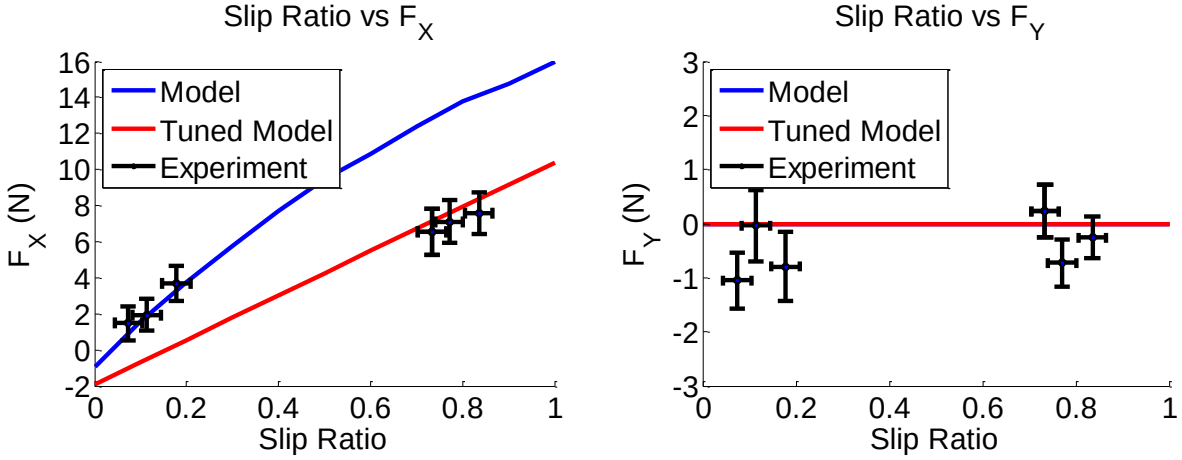

Fig. 7. *Single wheel test result at $\beta = 0°$*

5. Four Wheel Test

5.1 Rover Testbed Setup

To validate the simulator's output in an actual rover case, we have performed horizontal traversal test using the controlled sandbox environment (Fig. 8). We have simulated a sloped surface by tilting the testbed sideway, varying from ground to 20 degrees inclined angle. The rover's motion is tracked using the four motion capture cameras, and we have inserted 4 markers to determine the position and the attitude orientation at each time frame.

Fig. 8. *Four-wheel testbed setup and apparatus.*

5.2 Slope Traversal Test Result

The dynamic model is assessed as the following. We select the absolute reference frame of the rover's horizontal traversal direction to be along the inertial frame x_i axis. The sloped terrain is assumed to be flat and homogenous throughout the whole testing surface. Each wheel speed is set at 6 cm/s, and only forward movement is applied. The rover's mobility is studied in two cases. First, for each slope condition, we align the rover's attitude in parallel with the longitudinal direction to determine the absolute drift without any compensation technique. In second case, we align the rover's initial attitude to a specific γ. The initial angle is chosen based on the dynamic model's output for a successful horizontal traverse. Figure 9 shows the test result for the four inclined sloped conditions (α = 5°, 10°, 15°, 20°), and the resulting mean yaw angle is shown in Fig. 10. With an increase in testbed inclination angle, a gradual increase in side drift is observed when the rover moves in horizontal traversal direction. When the initial rover's attitude is pre-aligned, the passive drift correction reduced the side drift drastically for traversal run for every slope case, proving that the rover is capable of traversing a steep slope without any complicated active wheel control feedback. On the other hand, for the case of 20° slope, the rover's initial attitude from simulation did not match closely to the experiment. Therefore, a large increase in attitude angle was tested to achieve near horizontal traversal run. Based on the results, we determined that the simulation is reasonable to predict the traversal motion case of up to 15 degrees slope. The detailed error analysis is shown in Table 4.

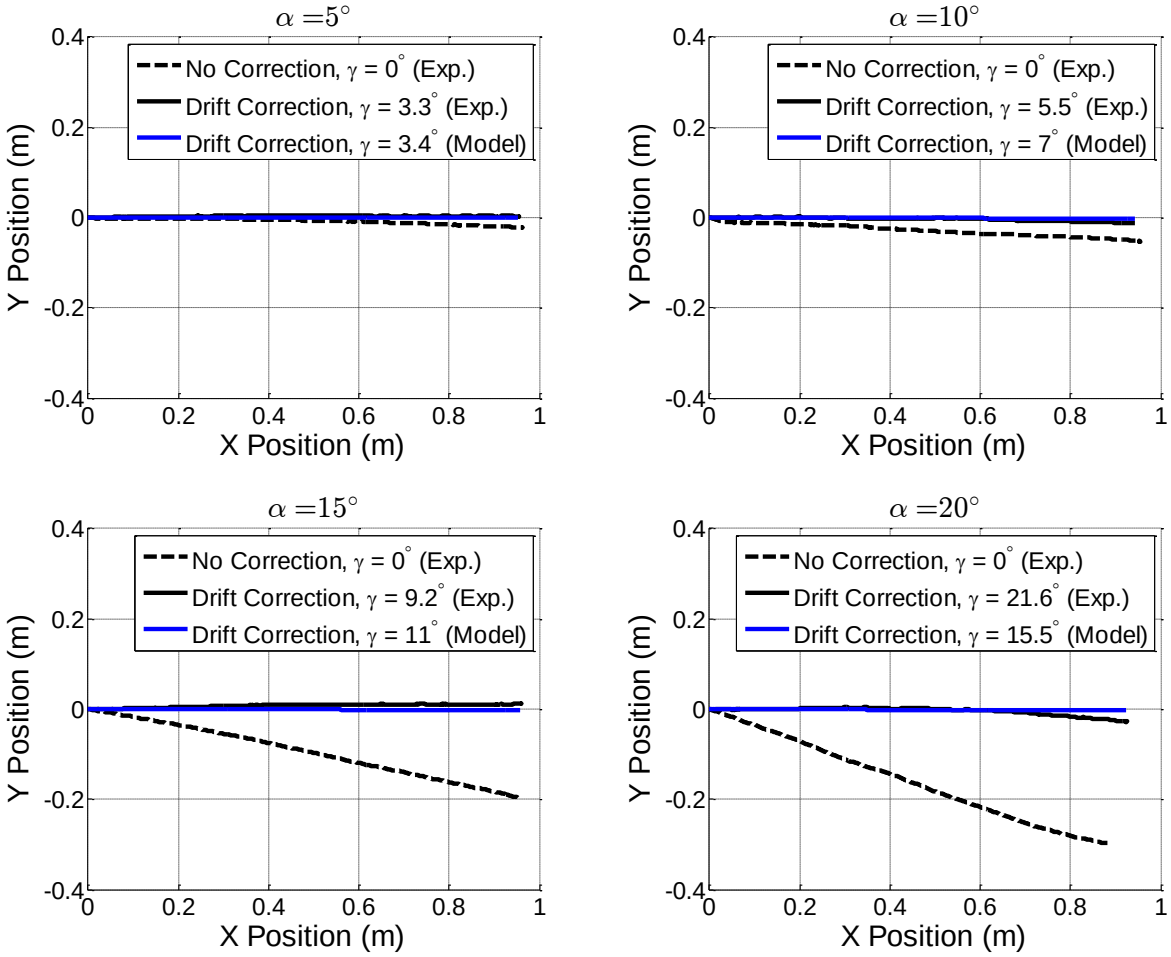

Fig. 9. *Four-wheel rover sandbox test results.*

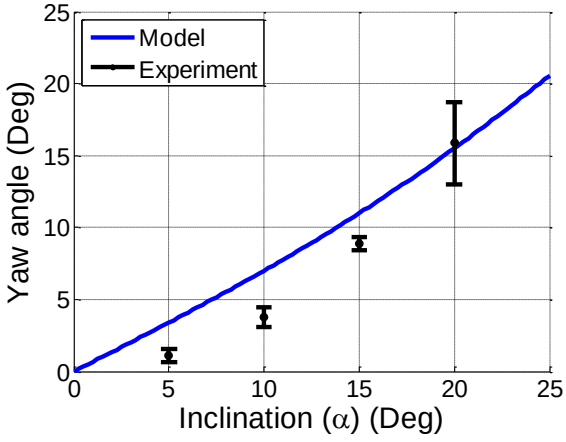

Fig. 10. *Slope-attitude correlation curve*

Table 4. Rms and final state errors on the compensated horizontal traversal run.

Slope		γ_{intial}	γ_{final}	γ_{inital} error (%)	γ_{final} error (%)	Distance Rms error	Final Distance error (m)
5	Model	3.4°	3.4°	-	-	-	-
	Experiment	3.31°	0.56°	2.40%	83.54%	3.57%	0.003
10	Model	5.5°	5.5°	-	-	-	-
	Experiment	5.51°	3.10°	0.10%	43.68%	6.00%	0.013
15	Model	11°	11°	-	-	-	-
	Experiment	9.19°	8.75°	16.45%	20.49%	8.83%	0.011
20	Model	15.5°	15.5°	-	-	-	-
	Experiment	21.63°	12.05°	39.56%	22.29%	13.34%	0.028

6. Conclusion

In this paper, we have discussed the dynamics model formulation of the micro-sized four-wheel rover in a sandy terrain condition. The dynamics are simplified under the condition that the rover's reference frame always stays in flat surface to minimize the rotational degree of freedom along the y_b-axis. We have successfully demonstrated that the rover is capable of traversing sloped terrain in a straight path up to 15 degrees by determining the optimal attitude-slope correlation based on the well-established terramechanics model. While the lunar conditions differ from the terrestrial environment, we can predict that the rover is presumably capable of horizontal traverse under slightly ramped surface during the actual mission. As a potential strategy to determine the attitude-slope relation curve during the lunar mission, we can conduct runs in several possible attitude orientations based on engineering intuition from terrestrial experimental results. Another option is to predict the initial attitude from the developed rover dynamics simulator using lunar environment condition such as gravity and regolith, which is the eventual goal of this work. The verification process will be by no means trivial due to the lack of apparatus available for ground truth in lunar surface. However, by utilizing the on-board inertial measurement unit and visual odometry to determine the instantaneous slope condition and traveled distance, we may be able to assess the near-fit attitude orientation for the straight locomotion in sloped terrain.

Future work will include an improvement on the rover's horizontal locomotion in an inclined slope of beyond 20 degrees. This can be done by implementation of independent speed control of each wheel in two methods; autonomously adjust the wheel velocity from experimental results or iterate the state vectors by measuring the instantaneous motor current output of the wheel to determine the slip in near real time. Another update that should be considered is the real-time visual odometry and terrain information to obtain accurate position information. Finally, the formulated dynamics simulator will be updated for the lunar environment case to forecast the rover's mobility performance in actual mission.

Nomenclature

a_0	Maximum stress angle modulus 0	-
a_1	Maximum stress angle modulus 1	-
c	Cohesion stress	[kPa]
d	Distance traveled	[m]
$\tilde{d}_i$	Constant distance vector	[m]
F_x	Longitudinal force	[N]
F_y	Lateral force	[N]
h	Wheel sinkage	[m]
h_g	Grouser height	[m]
k'_c	Soil destructive angle	-
k'_ϕ	Cohesive modulus	-
K_x	Longitudinal shear deformation modulus	m
K_y	Lateral shear deformation modulus	m
m	Mass	[kg]

M	Moment	[Nm]
N	Number of grouser	-
n	Sinkage exponent	-
s	Slip ratio	-
s_{ref}	Reference slip ratio	-
T	Torque	[Nm]
W	Normal load	[N]
X_c	Soil destructive angle	[Degrees]
v_x	Longitudinal velocity	[m/s]
v_y	Lateral velocity	[m/s]
α	Inclination angle	[Degrees]
β	Slip angle	[Degrees]
γ	Yaw angle	[Degrees]
θ_i	Wheel rotation angle	[Degrees]
ρ	Soil density	[kg/m^3]
ω	Angular velocity	[rad/s]
ϕ	Friction angle	[Degrees]

Acknowledgements

This research is partially funded by the Tohoku University Division for Interdisciplinary Advanced Research and Education.

References

Bekker, M.G., 1960. Off-the-road locomotion, The University of Michigan Press, Ann Arbor, Michigan..

Bekker, M.G., 1969. Introduction to Terrain-Vehicle Systems. University of Michigan Press, Ann Arbor, Michigan.

Fujii, K., Fujimoto, H., 2007. Traction Control based on Slip Ratio Estimation Without Detecting Vehicle Speed for Electric Vehicle. In Proceeding of the Power Conversion Conference, Nagoya, Japan, 688-693.

Inotsume, H., Creager, C., Wettergreen, D., Whittaker, W..R.., 2016. Finding routes for efficient and successful slope ascent for exploration rovers. In Proceedings of the International Symposium on Artificial Intelligence, Robotics and Automation in Space, Beijing, China.

Ishigami, G., Miwa, A., Nagatani, K., Yoshida, K., 2007. Terramechanics-based model for steering maneuver of planetary exploration rover on loose soil. Journal of Field Robotics. 24, 233-250.

Ishigami, G., Nagatani, K., Yoshida, K., 2009. Slope traversal controls for planetary exploration rover on sandy terrain. Journal of Field Robotics. 26, 264-286.

Irani, R.A., Bauer, R.J., Warkentin, A., 2011. A dynamic terramechanic model for small lightweight vehicles with rigid wheels and grousers operating in sandy soil. Journal of Terramechanics, Elsevier, 48, 307-318.

Janosi, Z., and Hanamoto, B., 1961. The analytical determination of drawbar pull as a function of slip for tracked vehicle in deformable soils. In Proceedings of the 1st International Conference on Terrain-Vehicle Systems, Torino, Italy.

Li, W., Ding, L., Gao, H., Deng, Z., Li, N., 2013. ROSTDyn: Rover simulation based on terramechanics and dynamics. Journal of Terramechanics. 50, 199-210.

Kerr, R.A., 2009. Mars rover trapped in sand, but what can end a mission? Science. 324, 998-998.

Merion-Griffith, G., Spenko, M., 2014. Simulation and experimental validation of a modified terramechanics model for small-wheeled vehicles. International Journal of Vehicle Design, 64, 153-169.

Nagaoka, K., Nakata, K., Higa, S., Yoshida, K., 2016. Mobility characteristics and control of a skid-steering micro-rover for planetary exploration on loose soil. In Proceedings of the International Symposium on Artificial Intelligence, Robotics and Automation in Space, Beijing, China.

Sutoh, M., 2013. Traveling performance analysis of lunar/planetary robots on loose soil. Ph.D. Thesis, Tohoku University, Sendai, Japan.

Sutoh, M., Nagaoka, K., Nagatani, K., Yoshida, K., 2013. Design of wheels with grousers for planetary rovers traveling over loose soil. Journal of Terramechanics, Elsevier, 50, 345-353.

Wong, J.Y., Reece, A.R., 1967. Prediction of rigid wheel performance based on the analysis of soil-wheel stresses part I. Performance of driven rigid wheels. Journal of Terramechanics. 4, 81-98.

Wong, J.Y., 2008. Theory of Ground Vehicle. John and Wiley & Son, Inc, Hoboken, New Jersey.